Received January 28, 2021, accepted February 23, 2021, date of publication February 26, 2021, date of current version March 26, 2021.

Digital Object Identifier 10.1109/ACCESS.2021.3062460

Dual Circularly Polarized Fabry–Perot Resonator Antenna Employing a Polarization Conversion Metasurface

YAWEN WANG AND ANXUE ZHANG
School of Information and Communications Engineering, Xi'an Jiaotong University, Xi'an 710049, China
Corresponding author: Anxue Zhang (anxuezhang@xjtu.edu.cn)

ABSTRACT A dual circularly polarized (CP) Fabry-Perot (FP) resonator antenna is presented in this paper. A linear to circular polarization conversion metasurface (MS) is employed as the superstrate of the FP resonator antenna. The working principle of the unit cell adopted by the MS enables it to independently control the transmission and reflection characteristics. Firstly, the MS is designed to present high reflectivity to ensure the high gain of the FP resonator antenna. Then the capability of polarization conversion is endowed to it. The square patch of the unit cell can receive two orthogonal LP waves, and the cross slot on the ground plane can also make them get through. Meanwhile, the circular patch with 45° tilted etched slot can radiate different CP waves when excited by different LP waves. Therefore, the proposed MS can combine the function of partial reflection and transmission polarization conversion. And for different LP waves, the MS can convert them into different CP waves. A dual LP microstrip patch antenna is designed to act as the feed of the resonator antenna. When the antenna is fed at different ports, different LP waves are excited in the resonant cavity and are converted into different CP waves by the MS, thus the antenna obtains dual CP radiation. The measured results indicate that the antenna can exhibit excellent dual CP radiation characteristic. Compared with other reported dual CP resonator antennas, the proposed antenna can obtain well performance with simple structure and low profile.

INDEX TERMS Dual circularly polarized, Fabry–Perot resonator antenna, polarization conversion metasurface, high gain.

I. INTRODUCTION

The circularly polarized antennas have been widely used in many communication systems due to their advantages of immunity to multipath effects and polarization mismatching. Among them, the dual CP antennas can change their polarizations according to the requirements. Therefore they have a wider range of applications [1]–[6]. A magneto-electric (ME) dipole antenna with dual CP radiation is proposed in [6]. The antenna is formed by two electric dipoles, two magnetic dipoles and two Γ-shaped feeds. The designed antenna can be used to realize frequency reuse and polarization diversity.

The CP antennas with high gain are required in many communication systems. The Fabry- Perot (FP) resonator antenna is a common type of high gain antennas [7]–[13]. It can generate high gain radiation depending on the resonant cavity formed by the superstrate and the ground plane. Fig. 1 shows the configuration of the FP resonator antenna. According to the ray tracing mode, the FP resonator antenna can obtain maximum gain in the boresight when the height of the cavity satisfies the following formula [14]:

$$h = \frac{\varphi_S + \varphi_G - 2N\pi}{4\pi}\lambda_0 \quad N = 0, 1, 2 \ldots \tag{1}$$

where λ_0 is the wavelength in the free space and φ_S and φ_G are the reflection phases of the superstrate and the ground plane, respectively. The FP resonator antenna can also be designed to obtain dual polarization [15]–[18]. The most used way to realize dual polarization FP resonator antenna is adopting dual polarized feed [19]–[21]. A dual-polarized dielectric resonant antenna is designed and used as the source of the FP resonator antenna in [19]. Combining with the proposed quad-layer partially reflection surface (PRS), the antenna can obtain dual polarization radiation in a wide operating band. There are also various reports about the dual CP FP resonator antenna [22]–[26]. In [24], a reconfigurable patch antenna is adopted as the feed of the FP resonator antenna, which can realize polarization configuration among

The associate editor coordinating the review of this manuscript and approving it for publication was Yasar Amin.

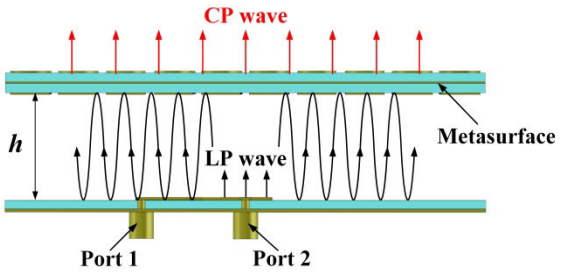

FIGURE 1. The working principle of the FP resonator antenna.

left handed circular polarization (LHCP), right handed circular polarization (RHCP) and linear polarization through changing the polarization of the feed antenna. A chiral MS is designed and employed as the superstrate of a FP resonator antenna in [25]. The MS can convert LP wave to different CP waves at different frequencies. So the formed FP resonator antenna can operate at dual band with dual-orthogonal circular polarization. By loading a LP to CP converter above the antenna, a dual CP FP resonator antenna is proposed in [26]. The antenna can radiate different CP waves when fed at different ports. However, this can make the antenna suffer from the disadvantages of complex structure and high profile. Besides, the wideband CP FP resonator antenna is also a huge challenge [27]. There are also many researches on the wideband CP FP resonator antenna.

In this paper, a linear to circular polarization conversion MS which can transform different linear polarizations to different circular polarizations is proposed to design a dual CP FP resonator antenna. A square patch is used to receive two orthogonal LP waves. Then the waves are coupled to a circular patch through a cross slot on the ground plane. The circular patch with a 45° tilted etched slot can radiate CP waves and generate different CP waves with different LP excitations. The reflection and transmission characteristics of the unit cell can be controlled independently. This makes the proposed MS combines the function of partially reflection and the polarization conversion. So it can act as the PRS and polarizer simultaneously. This will help the FP resonator antenna keep simple structure and low profile. A dual LP microstrip patch antenna is designed to behave as the feed of the resonator antenna. Then the high gain dual CP FP resonator antenna is realized. And it is also fabricated and measured. The measured results verify the correctness of the design.

The rest of the paper is organized as follows: the structure and characteristic of the proposed unit cell are presented in Section II. The design process of the dual CP FP resonator antenna is described in the Section III. The simulated and measured results of the proposed antenna are displayed in Section IV. Finally, the conclusion is drawn in Section V.

II. ANALYSIS OF THE PROPOSED UNIT CELL

A unit cell with the ability of linear to circular polarization conversion is proposed in this paper. The configuration of the unit cell is displayed in Fig. 2. It consists of two-layer substrates and three-layer metal structures. The substrates are

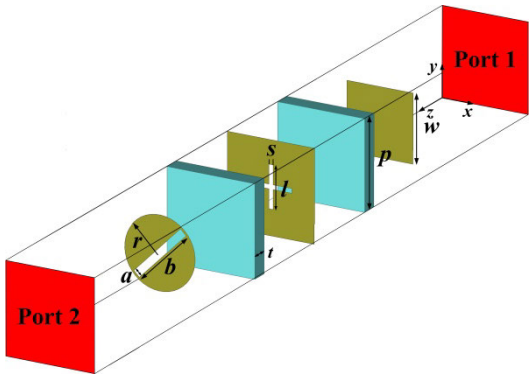

FIGURE 2. The configuration of the unit cell.

F4B with a thickness of 1.6 mm and the relative permittivity of 2.65. The loss tangent of the substrate is 0.002. The period of the unit cell is $p = 8$ mm. The bottom layer metal is a square patch and the top layer metal is a circular patch with a rectangle slot. While the middle layer metal is a ground plane with a cross slot. The incident wave is received by the square patch on the bottom layer and then coupled to the circular patch on the top layer through the slot on the middle layer. Then the circular patch radiates them into space. The square patch on the bottom layer can receive x- and y-polarized waves. The cross slot on the ground plane can also make two polarization waves get through and couple to the circular patch. The slot along x- axis can receive and couple y- polarized wave, while the slot along y- axis can receive and couple x- polarized one. Besides, the length of the slot influences the transmission magnitude of the unit cell, which enlarges with the increase of the slot length. The unit cell is designed to present high reflectivity firstly to ensure the high gain of the FP resonator antenna. The circular patch with the rectangle slot can be seen as a patch antenna fed by the slot on the ground plane. The angle between the orientation of the rectangular slot and the coordinate axis is 45°. This slot can make the circular patch radiate CP wave. Moreover, when the patch is fed by different slots, it can radiate CP waves with different rotations.

In order to explain the working principle of the unit cell more clearly, the equivalent transmission circuit of the unit cell is built, as shown in Fig. 3. The periodic square patch on the bottom layer can be equivalent to a capacitor and an

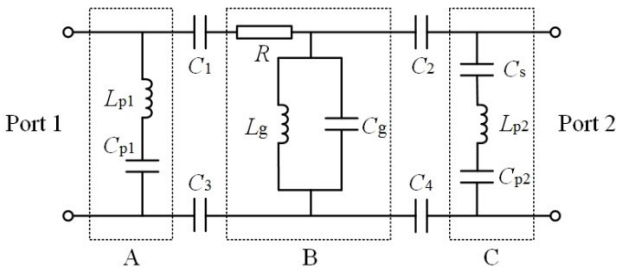

FIGURE 3. The equivalent transmission circuit of the unit cell.

inductor in series, as the C_{p1} and L_{p1} in the Part A. The C_{p1} is introduced by the edges of the two adjacent patches, while the L_{p1} is generated by the patch itself. So the inductance is very small. However, the periodic circular patch with rectangle slot on the top layer is equivalent to two capacitors and an inductor in series, as C_{p2}, L_{p2} and C_s in Part C. Similar to the periodic square patch on the bottom layer, the L_{p2} and C_{p2} are introduced by the patch and its edges, respectively. However, the capacitor (C_s) is introduced by the slot on the patch. Then the metal ground plane with cross slot in the middle layer is equivalent to a capacitor and an inductor in parallel, as the C_g and L_g in Part B. The resister R in part B represents impedance introduced by the slot on the ground plane. Besides, the capacitance between the patches and the ground plane can be represented by four capacitors between different parts.

In the simulation, the electromagnetic wave comes from port 1 and is received by port 2. Port 1 is set in the LP mode and port 2 is set in the CP mode. The mode 1 of port 1 is y- polarization and the mode 2 is x- polarization. While the mode 1 of port 2 is LHCP and the mode 2 is RHCP. The Fig. 4 shows the comparison between the simulation results and the calculated results of the equivalent circuit. The values of all parameters in the equivalent circuit are shown in Table 1. It can be found that, the full wave simulated results of the unit cell agree well with the calculated results of the equivalent circuit. Then the S parameters of the unit cell with different polarization incident waves are shown in Fig. 5 and Fig. 6. In the figures, the T_{ij} represents the transmission coefficients from the mode j of port 1 to the mode i of port 2. While the R_{ij} represents the reflection coefficient. Fig. 5 plots the S parameters of the unit cell when y- polarized wave is incident and Fig. 6 is that when x- polarized wave is incident. It can be found that, for different polarized waves, the unit cell always presents high co-polarization reflection magnitude and low cross-polarization reflection magnitude, which ensures that the resonator antenna obtains high gain and maintains good polarization purity in the resonant cavity. Meanwhile, the transmission coefficients imply that the unit cell can convert the y- polarized wave to RHCP wave and

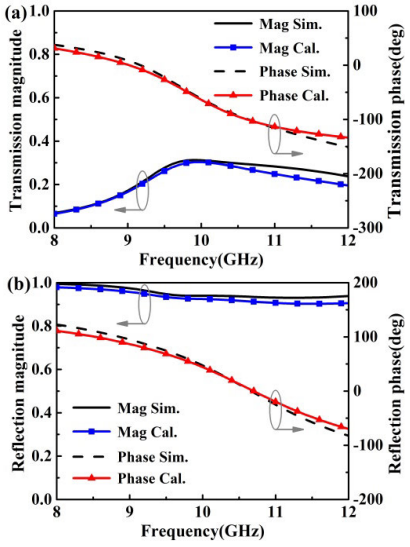

FIGURE 4. *S* parameters of the unit cell simulated by CST and calculated by the equivalent transmission circuit. (a) Transmission coefficients and (b) reflection coefficients.

TABLE 1. Approximate values of elements in equivalent circuit.

Element	C_{p1}(pF)	L_{p1}(nH)	C_g(pF)	L_g(nH)	R(Ω)
Value	0.71	2.0	1.6	0.6	195
Element	C_{p2}(pF)	L_{p2}(nH)	C_s(pF)	C_1(pF)	C_2(pF)
Value	0.67	2.0	0.71	0.38	0.39

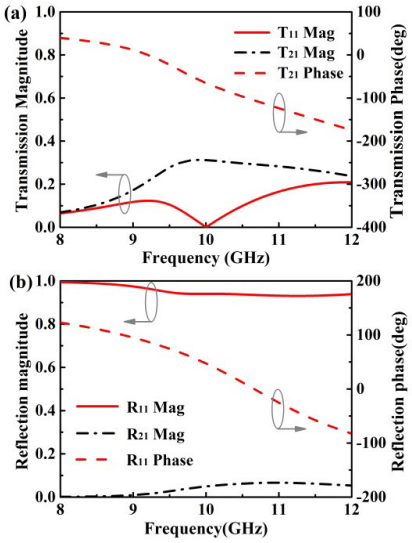

FIGURE 5. The simulated *S* parameters of the unit cell under *y*- polarized wave incidence. (a) Transmission coefficients and (b) reflection coefficients.

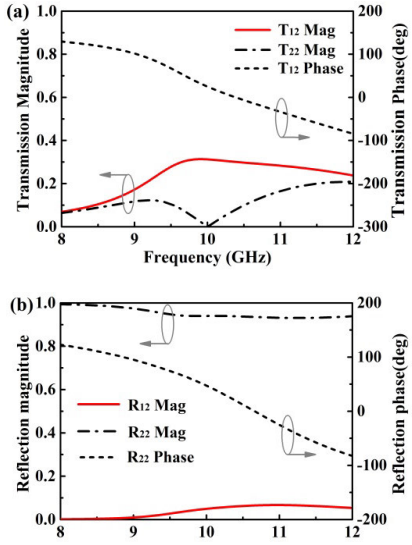

FIGURE 6. The simulated *S* parameters of the unit cell under *x*- polarized wave incidence. (a)Transmission coefficients and (b) reflection coefficients.

x- polarized wave to LHCP wave. So the MS formed by this unit cell can not only realize linear to circular polarization conversion, but also convert different LP waves into different CP waves.

The polarization conversion ratio of the unit cell is also investigated. The metasurface in this paper is designed to present high reflectivity (about 0.94) and the transmission magnitude is very small. So, the polarization conversion ratio can be calculated by:

$$\eta = \frac{T_{co}^2}{T_{co}^2 + T_{cross}^2} \tag{2}$$

which represents the ratio of the energy of the transmitted co-polarized wave to the total transmitted energy. The calculated results show that the polarization conversion ratio of the metasurface is large than 98% in the range of 9.8-10.2 GHz and reaches almost 1 at 10 GHz.

III. DESIGN OF POLARIZATION CONVERSION MS

A polarization conversion MS is formed by the proposed unit cell. On one hand, the metasurface is expected to be large to make the antenna obtain high gain property. Because the large metasurface can avoid the energy diffractions from the edge of the cavity. On the other hand, the aperture efficiency of the antenna goes down when if the metasurface is too large, because the energy at the edge of the cavity is very less and the unit cells at the edge of the metasurface have little contribution to the gain of the antenna. Therefore, the metasurface is determined to consist of 10×10 unit cells after comprehensive consideration. The top views of three layers of the MS are displayed in Fig. 7.

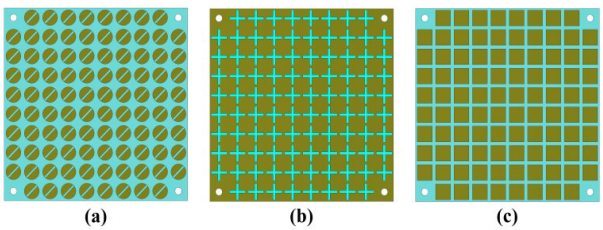

FIGURE 7. The views of three layers of the MS. (a) Top layer, (b) middle layer, and (c) bottom layer.

Four unit cells on the corners of the MS are removed, and four holes are added to facilitate the assembly of the antenna. The reflection and transmission coefficients of the MS are the same as the unit cell, which are demonstrated in Fig. 5 and Fig. 6. The total size of the MS is 80×80 mm^2.

A dual-polarized microstrip patch antenna is employed as the feed of the resonator antenna. Fig. 8 shows the configuration of the feed antenna. The substrate of the feed antenna is the same as the MS. A square patch on the top layer of the substrate is used as the radiator. Two ports and two feeding lines are adopted to feed the patch from different sides. Two SMA connectors connect two ports from the bottom side of the substrate. The impedance transforming lines are added into the feeding lines to achieve impedance matching.

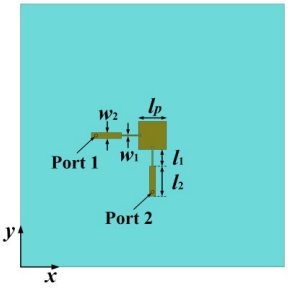

FIGURE 8. The schematic of the feed antenna.

When the antenna is fed by port 1, it radiates x- polarized wave and when the antenna is fed by port 2, it radiates y-polarized wave.

The FP resonator antenna is composed by the proposed MS and the designed dual-polarized feed antenna. The simulation model of the antenna in the CST is shown in Fig. 9. The MS is placed above the feed antenna with a distance of h, which is calculated according to the Eq. (1) and then optimized by the CST. The values of all parameters of the unit cell and the feed antenna are listed in Table 2.

TABLE 2. Parameters of the antenna.

Parameters	Value (mm)	Parameters	Value (mm)
p	8	t	1.6
w	6.5	r	3.25
l	4.8	s	0.2
a	6.4	b	0.75
lp	8.5	h	$\lambda_0/5$
w_1	0.4	w_2	1.8
l_1	5.1	l_2	9.15

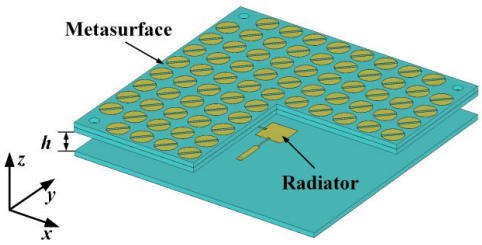

FIGURE 9. The simulation model of the dual CP FP resonator antenna.

IV. SIMULATED AND MEASURED RESULTS

Firstly, we give the simulated current distribution on the metasurface in Fig. 10. The four figures on top line are the current distributions when port 1 is fed with different phases and that on bottom line is the current distributions when port 2 is fed with different phases. It can be clearly seen that the antenna radiates LHCP waves when port 1 is fed and RHCP waves when port 2 is fed.

To validate the performance of the proposed antenna, a prototype antenna is fabricated and measured. The photographs of the fabricated antenna are displayed in Fig. 11. The antenna is measured in an anechoic chamber. The simulated and

TABLE 3. Comparison of the proposed antenna with previous reported works.

Ref.	Frequency (GHz)	Polarization mode	Profile (λ_0)	Method	Superstrate	Maximum Gain (dBi)	Aperture Efficiency	Aperture Size (λ_0)	Operating Bandwidth (GHz)
19	5.5	Dual LP	0.65	Dual feed	Double layer	15.5	63.5%	$2.1\lambda_0\times2.1\lambda_0$	5.05-5.8 (14.8%)
24	7.5	LP and dual CP	0.6	Reconfigurable feed	Single layer	15.1	41.2%	$2.5\lambda_0\times2.5\lambda_0$	7.3-7.6 (4%)
25	7.28 8	Dual CP at different frequency	0.55	Single feed	Single layer	12.98 13.25	38% 33.5%	$2.3\lambda_0\times2.3\lambda_0$	7.24-7.69 (1.1%) 7.96-8.14 (2.5%)
26	12.5	Dual CP	1.4	Dual feed	Double layer	12.8	24.3%	$2.5\lambda_0\times2.5\lambda_0$	12.07-13.25 (9.3%)
Proposed antenna	10	Dual CP	0.36	Dual feed	Single layer	13.4	24.5%	$2.6\lambda_0\times2.6\lambda_0$	9.86-10.14 (2.8%)

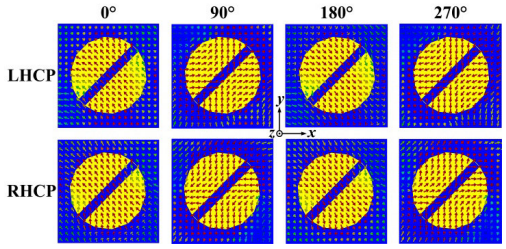

FIGURE 10. The current distribution on the metasurface.

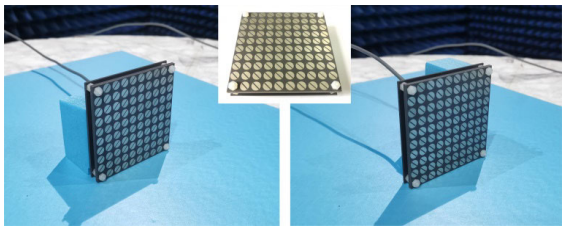

FIGURE 11. The photographs of the fabricated antenna and the experiment environment.

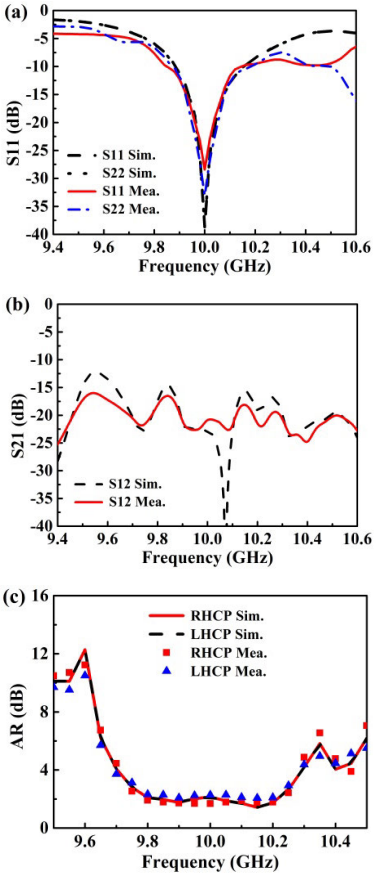

FIGURE 12. The simulated and measured results of the antenna. (a) Reflection coefficients, (b) port isolation, and (c) AR.

measured reflection coefficients and ARs versus frequency are plotted in Fig 12. The simulated reflection coefficients of port 1 and port 2 are exactly the same, because the structure of the antenna is rotationally symmetric. The measured reflection coefficients of two ports are not exactly the same, but the difference between them is very small. And they all agree well with the simulated results. The measured operating band, where reflection coefficient of the antenna is lower than −10 dB, is 9.86 – 10.14 GHz (2.8%). The isolation between two ports is also measured, which is displayed in Fig. 12 (b). The isolation between two ports is around −20 dB in the operating band. The measured ARs of LHCP and RHCP waves radiated by the antenna are plotted in Fig. 12 (c). The 3 dB AR bandwidth of the antenna is 9.75 – 10.25 GHz (5%), which is wider than the impedance bandwidth.

The radiation patterns of the antenna are measured and presented in Fig. 13 and Fig. 14. Fig. 13 exhibits the radiation patterns of the antenna fed by port 1. It is apparent that the antenna radiates the LHCP wave. The measured results indicate that the antenna obtains excellent radiation characteristic and the levels of the RHCP are lower than −20 dB. Likewise, the radiation patterns of the antenna fed by port 2 are presented in Fig. 14. The RHCP wave is radiated by the antenna in this time. And the levels of the LHCP are also lower than −20 dB. There are some differences between the measured side-lobe-levels (SLLs) and simulated results.

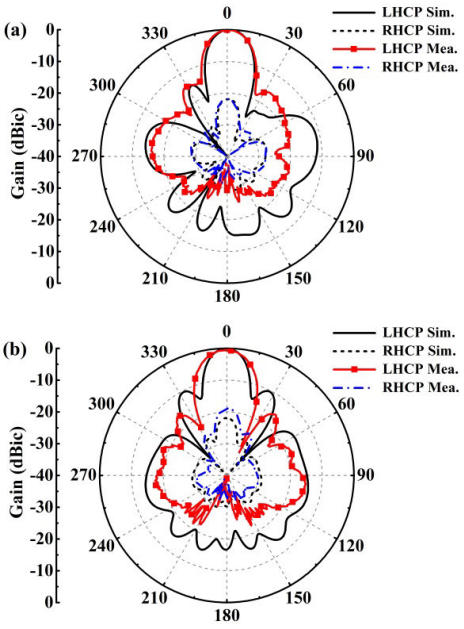

FIGURE 13. The radiation patterns of the antenna fed by port 1: (a) in plane $\varphi = 0°$, and (b) in plane $\varphi = 90°$.

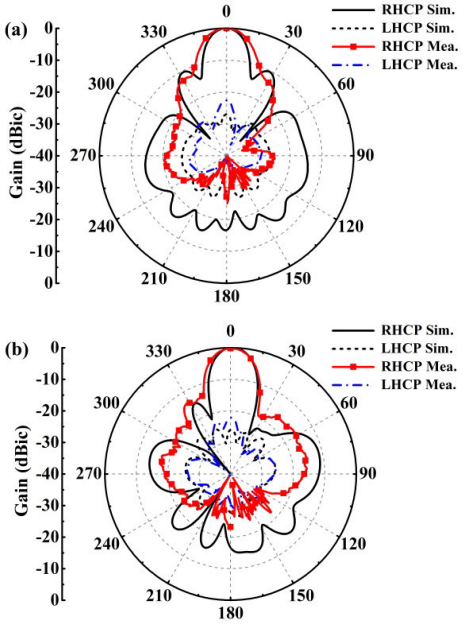

FIGURE 14. The radiation patterns of the antenna fed by the port 2: (a) in plane $\varphi = 0°$, and (b) in plane $\varphi = 90°$.

This may be caused by the test error. Besides, the AR of the antenna versus the angle are plotted in Fig. 15. The ARs of the antenna fed by both ports are all lower than 3 dB in the main beam range no matter when it working at RHCP or LHCP. The simulated and measured gain of the antenna is shown in Fig. 15 (a) and the calculated aperture efficiency of the antenna is shown in Fig. 15 (b). The realized gains of the antenna are the same when fed by different ports. The maximum gain of the antenna reaches 13.4 dBic for both CP

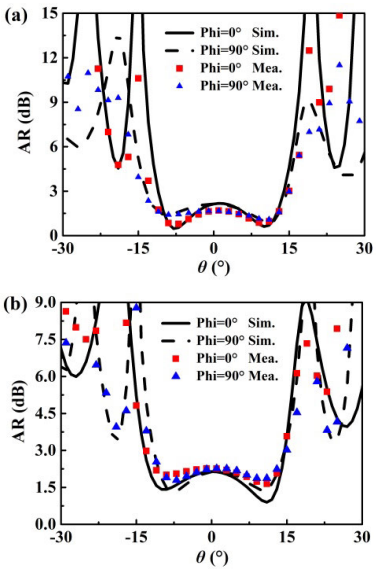

FIGURE 15. The AR of the antenna versus the angle. (a) Fed by port 1, and (b) fed by port 2.

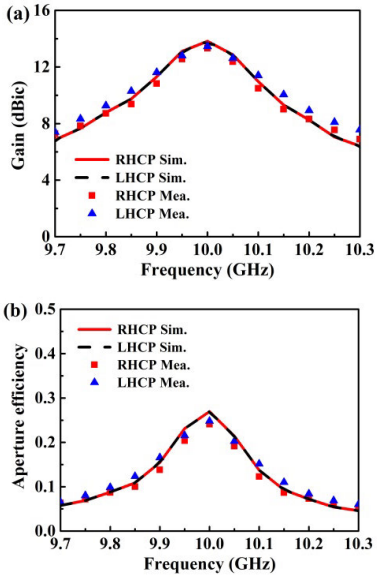

FIGURE 16. The simulated and measured gains and aperture efficiency of the antenna. (a) Gain, and (b) aperture efficiency.

waves. And the maximum measured aperture efficiency of the antenna reaches 24.5% at 10 GHz.

The comparison between the proposed antenna and other dual polarized resonator antennas is displayed in Table 3. The proposed antenna can obtain dual CP radiation at the same frequency with just one simple metasurface. This makes the resonator antenna maintain simple structure without sacrificing antenna performance. The proposed MS in this paper also make the CP-FP resonator antenna obtain very low profile. In conclusion, the FP resonator antenna proposed in this paper can obtain high gain dual CP radiation with simple structure and low profile.

V. CONCLUSION

A high gain dual CP FP resonator antenna based on a polarization conversion MS is proposed in this paper. Firstly, the unit cell adopted by the MS is designed to present high reflectivity to make the resonator antenna obtain high gain. Next, the LP to CP conversion property is endowed to the unit cell. For different LP waves, the unit cell can convert them into different CP waves. Then, a dual LP patch antenna is designed to act as the feed. It can radiate different LP waves when fed by different ports. Combing the proposed MS and feed antenna, dual CP FP resonator antenna is formed. The measured results show that the antenna can obtain superior performance. The proposed antenna can be employed in many applications, such as satellite communication and radio frequency identification.

REFERENCES

[1] Z. H. Jiang, Y. Zhang, and W. Hong, "Anisotropic impedance surface-enabled low-profile broadband dual- circularly polarized multibeam reflectarrays for *Ka*-band applications," *IEEE Trans. Antennas Propag.*, vol. 68, no. 8, pp. 6441–6446, Aug. 2020.

[2] P. Naseri and S. V. Hum, "A dual-band dual-circularly polarized reflectarray for *K*/*Ka*-band space applications," in *Proc. 13th Eur. Conf. Antennas Propag. (EuCAP)*, Krakow, Poland, 2019, pp. 1–5.

[3] W.-L. Guo, G.-M. Wang, W.-Y. Ji, Y.-L. Zheng, K. Chen, and Y. Feng, "Broadband spin-decoupled metasurface for dual-circularly polarized reflector antenna design," *IEEE Trans. Antennas Propag.*, vol. 68, no. 5, pp. 3534–3543, May 2020.

[4] P. Naseri, J. R. Costa, S. A. Matos, C. A. Fernandes, and S. V. Hum, "Equivalent circuit modeling to design a dual-band dual linear-to-circular polarizer surface," *IEEE Trans. Antennas Propag.*, vol. 68, no. 7, pp. 5730–5735, Jul. 2020.

[5] D. K. Singh, B. K. Kanaujia, S. Dwari, and G. P. Pandey, "Modeling of a dual circularly polarized capacitive-coupled slit-loaded truncated microstrip antenna," *J. Comput. Electron.*, vol. 19, no. 4, pp. 1564–1572, Dec. 2020.

[6] W. Chen, Z. Yu, J. Zhai, and J. Zhou, "Developing wideband dual-circularly polarized antenna with simple feeds using magnetoelectric dipoles," *IEEE Antennas Wireless Propag. Lett.*, vol. 19, no. 6, pp. 1037–1041, Jun. 2020.

[7] P. Xie, G. Wang, H. Li, and J. Liang, "A dual-polarized two-dimensional beam-steering Fabry–Pérot cavity antenna with a reconfigurable partially reflecting surface," *IEEE Antennas Wireless Propag. Lett.*, vol. 16, pp. 2370–2374, 2017.

[8] B. A. Zeb and K. P. Esselle, "High-gain dual-band dual-polarised electromagnetic band gap resonator antenna with an all-dielectric superstructure," *IET Microw., Antennas Propag.*, vol. 9, no. 10, pp. 1059–1065, Jul. 2015.

[9] Y.-M. Cai, K. Li, W. Li, S. Gao, Y. Yin, L. Zhao, and W. Hu, "Dual-band circularly polarized transmitarray with single linearly polarized feed," *IEEE Trans. Antennas Propag.*, vol. 68, no. 6, pp. 5015–5020, Jun. 2020.

[10] F. Qin, S. Gao, G. Wei, Q. Luo, and C. Mao, "Wideband circularly polarized Fabry–Perot antenna [antenna applications corner]," *IEEE Antennas Propag. Mag.*, vol. 57, no. 5, pp. 127–135, Oct. 2015.

[11] Y. Cheng and Y. Dong, "Bandwidth enhanced circularly polarized Fabry–Perot cavity antenna using metal strips," *IEEE Access*, vol. 8, pp. 60189–60198, 2020.

[12] N. Hussain, M.-J. Jeong, J. Park, and N. Kim, "A broadband circularly polarized Fabry–Perot resonant antenna using a single-layered PRS for 5G MIMO applications," *IEEE Access*, vol. 7, pp. 42897–42907, 2019.

[13] N. Hussain, S. I. Naqvi, W. A. Awan, and T. T. Le, "A metasurface-based wideband bidirectional same-sense circularly polarized antenna," *Int. J. RF Microw. Comput.-Aided Eng.*, vol. 30, no. 8, Aug. 2020, Art. no. e22262.

[14] G. V. Trentini, "Partially reflecting sheet arrays," *IRE Trans. Antennas Propag.*, vol. 4, no. 4, pp. 666–671, Oct. 1956.

[15] F. Qin, S. S. Gao, Q. Luo, C.-X. Mao, C. Gu, G. Wei, J. Xu, J. Li, C. Wu, K. Zheng, and S. Zheng, "A simple low-cost shared-aperture dual-band dual-polarized high-gain antenna for synthetic aperture radars," *IEEE Trans. Antennas Propag.*, vol. 64, no. 7, pp. 2914–2922, Jul. 2016.

[16] F. Qin, S. Gao, G. Wei, Q. Luo, and J. Xu, "Array-fed dual-polarized wideband Fabry–Perot antenna based on metasurface," *Microw. Opt. Technol. Lett.*, vol. 58, no. 10, pp. 2316–2321, Oct. 2016.

[17] M. W. Niaz, Y. Yin, S. Zheng, and Z. Zhao, "Dual-polarized low sidelobe Fabry–Perot antenna using tapered partially reflective surface," *Int. J. RF Microw. Comput.-Aided Eng.*, vol. 30, no. 3, Mar. 2020, Art. no. e22070.

[18] Y.-H. Lv, X. Ding, and B.-Z. Wang, "Dual-wideband high-gain Fabry–Perot cavity antenna," *IEEE Access*, vol. 8, pp. 4754–4760, 2020.

[19] P.-Y. Qin, L.-Y. Ji, S.-L. Chen, and Y. J. Guo, "Dual-polarized wideband Fabry–Perot antenna with quad-layer partially reflective surface," *IEEE Antennas Wireless Propag. Lett.*, vol. 17, no. 4, pp. 551–554, Apr. 2018.

[20] S. S. Vinnakota, R. Kumari, and B. Majumder, "Dual-polarized high gain resonant cavity antenna for radio frequency energy harvesting," *Int. J. RF Microw. Comput.-Aided Eng.*, vol. 29, no. 12, p. 22003, Dec. 2019.

[21] T. Debogovic, J. Bartolic, and J. Perruisseau-Carrier, "Dual-polarized partially reflective surface antenna with MEMS-based beamwidth reconfiguration," *IEEE Trans. Antennas Propag.*, vol. 62, no. 1, pp. 228–236, Jan. 2014.

[22] L. Wen, S. Gao, Q. Luo, W. Hu, and Y. Yin, "Wideband dual circularly polarized antenna for intelligent transport systems," *IEEE Trans. Veh. Technol.*, vol. 69, no. 5, pp. 5193–5202, May 2020.

[23] Z. Guo, X. Cao, J. Gao, H. Yang, and L. Jidi, "A novel composite transmission metasurface with dual functions and its application in microstrip antenna," *J. Appl. Phys.*, vol. 127, no. 11, Mar. 2020, Art. no. 115103.

[24] H. H. Tran and H. C. Park, "A simple design of polarization reconfigurable Fabry–Perot resonator antenna," *IEEE Access*, vol. 8, pp. 91837–91842, 2020.

[25] C. Chen, Z.-G. Liu, H. Wang, and Y. Guo, "Metamaterial-inspired self-polarizing dual-band dual-orthogonal circularly polarized Fabry–Pérot resonator antennas," *IEEE Trans. Antennas Propag.*, vol. 67, no. 2, pp. 1329–1334, Feb. 2019.

[26] R. Huang, Z. Wang, G. Li, C. Lin, Y. Ge, and J. Pu, "A metasurface-enabled wideband high-gain dual-circularly-polarized Fabry–Perot resonator antenna," *Microw. Opt. Technol. Lett.*, vol. 62, no. 10, pp. 3195–3202, Oct. 2020.

[27] J. A. Sheersha, N. Nasimuddin, and A. Alphones, "A high gain wideband circularly polarized antenna withasymmetric metasurface," *Int. J. RF Microw. Comput. Aided Eng.*, vol. 29, no. 7, 2019, Art. no. e21740.

YAWEN WANG was born in Xi'an, Shaanxi, China. She is currently pursuing the bachelor's degree with Xi'an Jiaotong University. Her main research interests include metasurface antennas and mm-wave antenna design.

ANXUE ZHANG received the B.S. degree in electrical engineering from Henan Normal University, in 1996, and the M.S. and Ph.D. degrees in electromagnetic and microwave engineering from Xi'an Jiaotong University, in 1999 and 2003, respectively. He is currently a Professor with Xi'an Jiaotong University. His main research interests include metamaterials, RF and microwave circuit design, antennas, and electromagnetic wave propagation.